

Tyrosinase-Based Reporter Gene for Photoacoustic Imaging of MicroRNA-9 Regulated by DNA Methylation in Living Subjects

Haifeng Zheng,^{1,3} Lin Zhou,^{1,3} Yaru Shi,¹ Jie Tian,^{1,2} and Fu Wang¹

¹Engineering Research Center of Molecular and Neuro Imaging, Ministry of Education, School of Life Science and Technology, Xidian University, Xi'an, Shaanxi 710071, China; ²CAS Key Laboratory of Molecular Imaging, Institute of Automation, Chinese Academy of Sciences, Beijing 100190, China

MicroRNAs (miRNAs) are a class of negative regulators of gene expression and play critical roles in various biological processes. Conventional approaches for detecting miRNAs, such as northern blotting, microarray, and real-time PCR, usually require the lysis of cell samples and could not provide the *in vivo* information about miRNAs in living organisms. Here, we designed a tyrosinase (TYR)-based reporter to monitor miR-9 expression that is regulated by DNA methylation in living cells and animals. During DNA methylation of A549 cells treated by 5-aza-2'-deoxycytidine (5-Aza-dC), the CMV/TYR-3xTS reporter-transfected cells demonstrated a gradual decrease in melanin content, TYR activity, and photoacoustic signal because of the gradual activation of miR-9 expression. The miR-9-regulated repression of TYR activity also resulted in a significant decrease in photoacoustic signal from the flank of mice with 5-Aza-dC treatment, whereas the bioluminescence signal from internal control had no obvious change. The TYR-based miRNA reporter may serve as a new imaging probe for monitoring the dynamic expression of miRNAs during various cellular or disease progression in cells and living animals.

INTRODUCTION

MicroRNAs (miRNAs) are a class of small noncoding RNAs of approximately 22 nucleotides that regulate gene expression at the post-transcriptional level.¹ Through perfectly or imperfectly base-pairing with the 3' UTR of their target mRNA sequences, miRNAs resulted in the mRNA degradation or translation inhibition in a wide variety of biological processes including cellular proliferation, metabolism, and carcinogenesis.² miRNAs are frequently dysregulated in various cancers. Several overexpressed miRNAs function as oncogenes, whereas some downregulated miRNAs function as tumor suppressor genes.^{3,4} Among the several miRNAs, miR-9 is initially found to be specially expressed in neurogenesis⁵ and also shows tumor suppressor activity in cancer cells.^{6,7} Moreover, miR-9 methylation has been observed in 65% of primary non-small-cell lung cancer (NSCLC) patients and may serve as a prognostic parameter in patients.⁸ DNA methylation refers to the covalent addition of a methyl group to the 5' carbon of cytosines within cytosine-guanine dinucleotides and is identified as a mechanism leading to downregulation of miRNA genes in cancer cells.⁹ Methylation could be revers-

ible by demethylating drugs, such as DNA methyltransferase inhibitor 5-aza-2'-deoxycytidine (5-Aza-dC), which is able to cause gene reexpression.¹⁰ A comprehensive of miRNAs have been found to be regulated by DNA methylation after 5-Aza-dC treatment in cancers.¹¹

Given the important role of miRNAs in diverse biological processes, lots of approaches have been developed to detect the expression of miRNAs, such as northern blotting, real-time PCR, and microarray assays. However, these conventional methods usually require the lysis or fixation of cells and could not reflect miRNA activity in living organisms. Molecular imaging has emerged as a noninvasive technique and has been widely applied to monitor miRNA expression in living subjects by the employment of fluorescence protein, luciferase, or molecular beacon (MB).¹² One of the molecular imaging approaches is to utilize reporter genes by transfecting them into cells and tracking the signal of grafted cells in living animals. Based on the theory of miRNA hybridization with its target mRNA, our group previously developed a dual modality reporter gene system to visualize miR-16 expression, which was stimulated by chemoresistance drugs in gastric cancer cells and xenografted mice.¹³ In this dual reporter gene system, a radioisotope reporter, human sodium iodide symporter (hNIS), and a bioluminescent reporter, firefly luciferase (Fluc), were ligated to generate a fused protein hNIS/Fluc, which can be used for ^{99m}Tc-pertechnetate radionuclide imaging and bioluminescence imaging (BLI). Although this dual reporter gene successfully provided the *in vivo* imaging information about miRNA function with high sensitivity, it still suffered from some limitations, such as relatively large molecular size to be transfected or transduced into cells, and different substrates for each imaging modality.

Received 14 December 2017; accepted 22 January 2018;
<https://doi.org/10.1016/j.omtn.2018.01.008>.

³These authors contributed equally to this work.

Correspondence: Fu Wang, Engineering Research Center of Molecular and Neuro Imaging, Ministry of Education, School of Life Science and Technology, Xidian University, Xi'an, Shaanxi 710071, China.
E-mail: fwang@xidian.edu.cn

Correspondence: Jie Tian, CAS Key Laboratory of Molecular Imaging, Institute of Automation, Chinese Academy of Sciences, Beijing 100190, China.
E-mail: jie.tian@ia.ac.cn



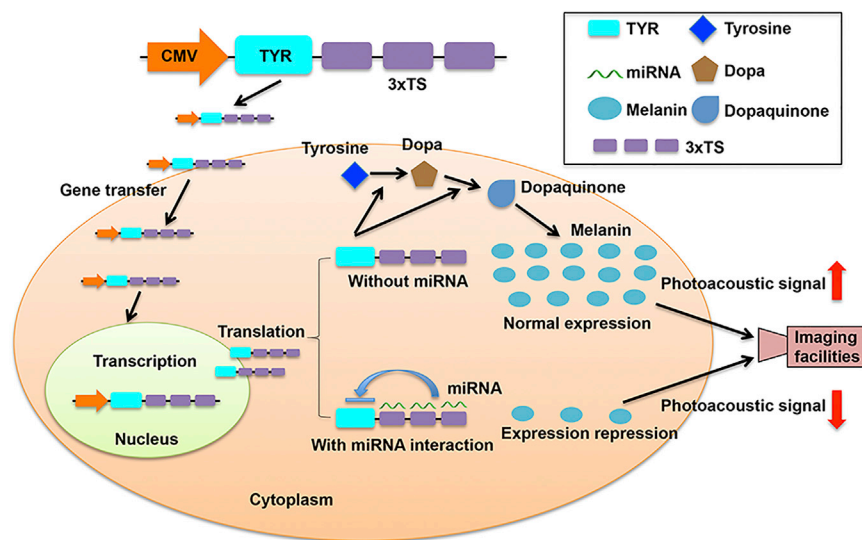


Figure 1. Schematic of the TYR-Based Reporter Gene System

CMV/TYR-3xTS reporter is regulated by CMV promoter and carries three copies of the target sequence complementary to miRNA-9 in its 3' UTR. The CMV/TYR-3xTS reporter gene is introduced into cells through gene transfer. After transcription and translation of the reporter, gene expression product tyrosinase catalyzes the oxidation of tyrosine and Dopa to synthesize melanin. Melanin then serves as a functional target for photoacoustic imaging (PAI). In the absence of miRNA in cells, the CMV/TYR-3xTS reporter gene is expressed normally. In contrast, when the miRNA is present in cells, the expression of reporter will be inhibited because of the interaction with miRNA, leading to the decreasing melanin content and finally reductive PAI signal.

Therefore, there have been urgent needs to develop alternative reporter genes to monitor the dynamic expression of miRNAs.

In the present study, we designed a tyrosinase (TYR) reporter gene to detect miR-9 involved in the regulation of DNA methylation in live cells and animals. TYR is the primary enzyme responsible for the production of melanin, which can provide strong absorption contrast for photoacoustic imaging (PAI) even in non-melanogenic cells.¹⁴ We demonstrated the feasibility of this TYR reporter for visualizing miR-9 activity, which could be reflected by the melanin content, TYR enzyme activity, and PAI signal both *in vitro* and *in vivo*.

RESULTS

Design of a TYR Reporter-Based miRNA Imaging System

To noninvasively monitor miR-9 expression in living cells and animals, we constructed a TYR-based reporter gene system, which was under the regulation of a cytomegalovirus (CMV) promoter. Three copies of perfectly complementary target sequences (3xTS) against miR-9 were inserted into the 3' UTR of the TYR vector to generate the CMV/TYR-3xTS reporter (Figure 1). Meanwhile, a CMV/TYR reporter that contains no 3xTS was also constructed as a control. When the CMV/TYR-3xTS reporter is introduced into cells by gene transfer, the expressed TYR will catalyze the process in melanin synthesis. The resulted gene product, melanin, can be served as a target for PAI. In the absence of miR-9, the TYR activity in cells is normally expressed because of no function of miR-9. In contrast, when endogenous or exogenous miR-9 is expressed in cells, miR-9 would bind to the 3xTS region of the CMV/TYR-3xTS reporter gene, resulting in the repression of TYR activity and melanin production, and thus the reduction of photoacoustic signals, which could be detected by a PAI system.

Characterization of TYR-Based Reporter Gene System

To characterize the TYR-based reporter gene system, we transfected non-melanocytic HEK293 cells, where miR-9 expression is relatively

low, with the CMV/TYR or co-transfected them with CMV/TYR-3xTS and miR-9 or negative control (NC) RNA. The pellets of transfected cells were then harvested to observe their color and melanin content. As shown in Figure 2A (upper row), the CMV/TYR transfected or CMV/TYR-3xTS and NC co-transfected cells exhibited dark colors, whereas CMV/TYR-3xTS and miR-9 co-transfected cells or 293 mock-transfected cells showed light colors, indicating that exogenous miR-9 bound to the 3xTS region of CMV/TYR-3xTS and repressed the expression of TYR gene. Moreover, pretreatment of the CMV/TYR- or CMV/TYR-3xTS-transfected cells with L-tyrosine (2 mM) for 24 hr significantly strengthened their color but had no obvious change in 293 mock-transfected cells, attributing to the oxidation of tyrosine by TYR to synthesize melanin in TYR-expressing cells (Figure 2A, lower row).

Consistent with the visual observation, quantification analysis of melanin content from these cells at 405-nm absorbance demonstrated that the melanin production was also increased in cells treated with L-tyrosine, with an exception of 293 mock-transfected cells (Figure 2B). The TYR activities in those transfected cells were also assessed by incubating the cell lysates with 1 mg/mL L-DOPA for different time points. It was shown that TYR activities, which were reflected by the amounts of dopachrome produced, in CMV/TYR-transfected or CMV/TYR-3xTS and NC co-transfected cells were increased over time and significantly higher than that of 293 mock-transfected or CMV/TYR-3xTS and miR-9 co-transfected cells (Figure 2C). These results demonstrated the successful construction of CMV/TYR-3xTS reporter gene as an miRNA imaging system in response to miR-9 function.

Specificity of TYR-Based Reporter Gene for Imaging of miR-9

To investigate the specificity of the TYR-based reporter gene, we transfected different amounts (0, 1, 2, 4 μ g) of CMV/TYR or CMV/TYR-3xTS plasmids into 293 cells. The cell pellets were then collected to examine their color and melanin content. The gradual increased introduction of plasmids into cells resulted in a significantly gradual

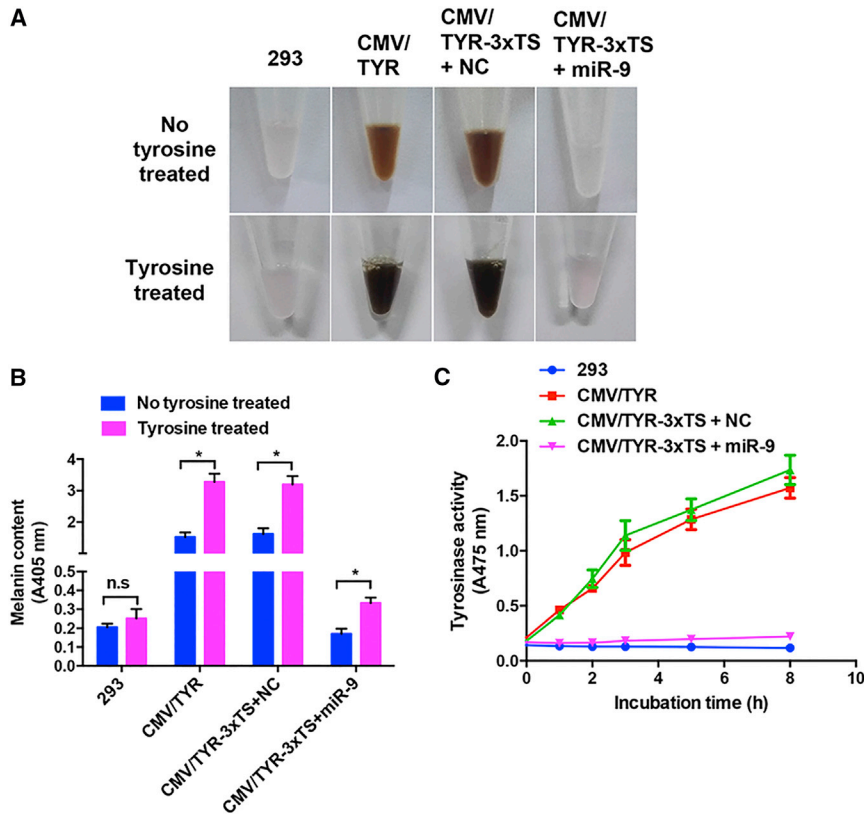


Figure 2. Characterization of TYR-Based Reporter Gene System

HEK293 cells were transfected with the CMV/TYR or co-transfected with CMV/TYR-3xTS and miR-9 or negative control (NC) RNA. (A) Photos of the cell pellets from 293 cells alone and the transfected cells without (upper) or with (lower) 2 mM L-tyrosine treatment for 24 hr. (B) Melanin production in 293 cells alone and the transfected cells without or with 2 mM L-tyrosine treatment for 24 hr. (C) Time-response tyrosinase activity curves in 293 cells alone and the transfected cells as above. Data are presented as means \pm SD (* $p < 0.05$).

increase in dark colors (Figure 3A) and melanin production (Figure 3B) in both CMV/TYR- and CMV/TYR-3xTS-transfected groups. Moreover, the TYR activities in both groups were also increased in a dose-dependent manner by measuring the absorbance of dopachrome at 475 nm (Figure 3C). We then detected the photoacoustic signal from the bottom of tubes containing cell samples. Quantitative analysis demonstrated that photoacoustic signal was increased according to the increased amounts of CMV/TYR-3xTS plasmids (Figure 3D). The gradual increase in melanin content and TYR activities, as well as photoacoustic signal, is mainly due to the increased gene expression of TYR, which is regulated by the CMV promoter and barely inhibited by miR-9 in 293 cells.

In contrast, with introduction of increased concentrations of exogenous miR-9 (0, 5, 10, 20, 40 nM) and a fixed amount (4 μ g) of CMV/TYR-3xTS plasmids in 293 cells, the cell colors were getting lighter gradually (Figure 4A). Besides, a significantly gradual decrease was also observed in the melanin content (Figure 4B), TYR activity (Figure 4C), and photoacoustic intensity (Figure 4D), indicating that the hybridization of exogenous miR-9 with the 3xTS region in the CMV/TYR-3xTS reporter resulted in the destabilization of TYR mRNA, and thus the repressed activity of TYR.

Monitor Endogenous miR-9 during DNA Methylation Regulation

To visualize the expression of endogenous miR-9 during DNA methylation regulation in cancers using the TYR-based reporter, we

transfected A549 NSCLC cells with the CMV/TYR-3xTS and further treated them with different concentrations (0, 0.5, 1, 2 μ M) of a DNA methyltransferase inhibitor 5-Aza-dC for 72 hr. The digital photos showed that the cell colors were getting lighter gradually according to increased dose of 5-Aza-dC (Figure 5A). Moreover, the melanin content (Figure 5B), TYR activity (Figure 5C), and photoacoustic signal (Figure 5D) were also gradually decreased in a dose-dependent manner after 5-Aza-dC treatment. The decrease was probably attributed to the fact that 5-Aza-dC activated the expression of endogenous miR-9, which resulted in the inhibition of TYR activity gradually. To confirm our speculation, we performed real-time PCR assay to determine the expression level of miR-9 in cells treated by 5-Aza-dC. As expected, the miR-9 was found to be upregulated gradually with the increased dose of 5-Aza-dC (Figure 5E).

In Vivo Imaging of miR-9 Using the TYR-Based Reporter

To monitor miR-9 expression during epigenetic gene regulation using the TYR-based reporter system *in vivo*, we co-transfected the CMV/TYR-3xTS reporter into 5×10^6 A549 cells with a Fluc plasmid pGL3-control, which was used as an internal control. Then the cell-incorporated Matrigels were subcutaneously implanted into both flanks of a nude mouse. Only the A549 cells grafted into the right flank received 5-Aza-dC treatment. The photoacoustic images from the mouse bearing the A549 cells were acquired after treatment for 3 days. As shown in Figure 6A, the photoacoustic signal from the right flank of mice treated with 5-Aza-dC was significantly decreased comparing with that from the left flank. Quantification analysis of region of interest (ROI) demonstrated that the fold change of photoacoustic intensity from the right flank was 1.54-fold lower than that from the left flank (Figure 6B).

In contrast, the bioluminescence signals from the internal control of pGL3-control, which constantly expresses the luciferase regardless of the presence of miR-9 during 5-Aza-dC treatment, have no obvious change between the left flank and right flank, indicating that equal numbers of cells were implanted and survived in both flanks for

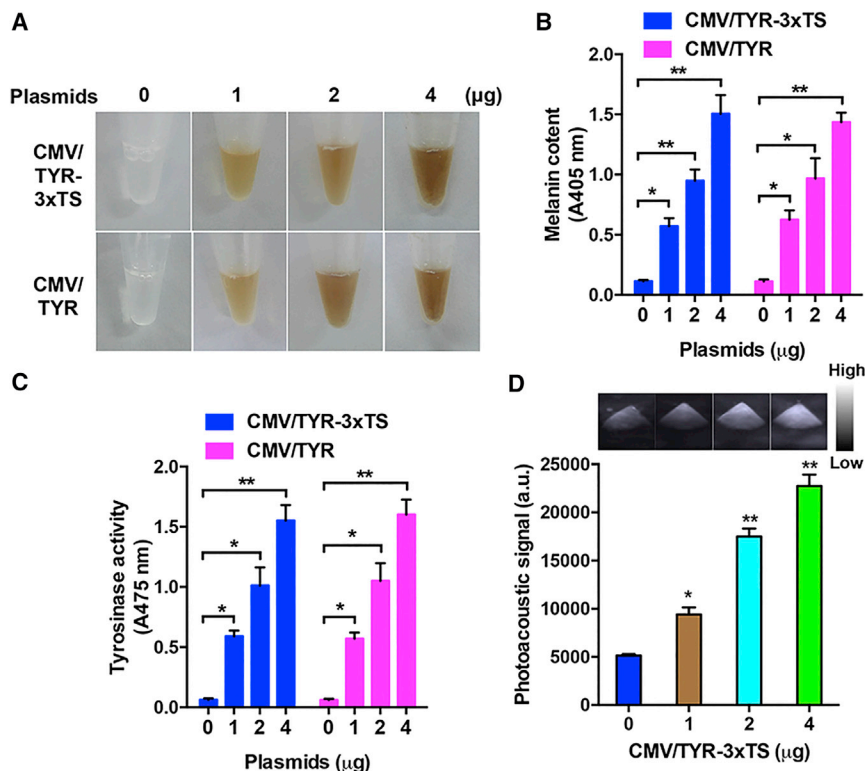


Figure 3. Dose-Response Assessment of the TYR-Based Reporter Gene

Different amounts (0, 1, 2, 4 µg) of CMV/TYR or CMV/TYR-3xTS plasmids were transfected into 293 cells, and the cell pellets were collected to examine the (A) color change, (B) melanin content, (C) tyrosinase activity, and (D) photoacoustic intensity. Data are presented as means \pm SD (* p < 0.05, ** p < 0.01 compared with control).

ground because of external light sources. Compared with the existing optical imaging modalities, PAI enables production of *in vivo* 3D images with higher spatial resolution (up to 500 µm at tissue penetration depth of about 5 cm).^{19,20} The underlying mechanism is involved in the transformation from the absorption of light in samples to the ultrasound. Due to the unique property of melanin as an excellent endogenous PAI contrast agent,^{21,22} TYR, the modulator of melanin synthesis, has been recently developed as a reporter gene for PAI in cells and xenograft tumors.^{14,23} Moreover, by chelating melanin with metal ions (e.g., Fe³⁺) or introducing the melanin avid probe (e.g., ¹⁸F-P3BZA), TYR has been utilized as a dual or multifunctional reporter gene for mag-

netic resonance imaging (MRI), positron emission tomography (PET), and PAI *in vitro* and *in vivo*.^{24–26} However, in the aforementioned studies, TYR was only validated as a reporter gene for PAI single-modality imaging or PAI/MRI/PET multimodality imaging; the potential application of TYR in visualizing gene expression was not fully investigated.

We designed a TYR-based miRNA reporter by inserting three complementary sequences against miR-9 into the 3' UTR of TYR gene. Our TYR reporter could provide *in vivo* information about miRNA function under various regulations and repeat on the same subjects noninvasively. In A549 cells treated with 5-Aza-dC, the TYR activity from the CMV/TYR-3xTS reporter was obviously inhibited by the increased dose of functional miR-9, which targets the complementary sequences in the 3' UTR of the CMV/TYR-3xTS gene. The miR-9-regulated repression of TYR activity also resulted in a clear decrease in melanin content and photoacoustic signal *in vitro* and *in vivo*. Additionally, the gradual decrease was also observed in the CMV/TYR-3xTS-transfected cells after 5-Aza-dC treatment. The result implies that the expression of miR-9 was activated by 5-Aza-dC, and thus inhibited the TYR activity and photoacoustic signal through hybridizing with its target sequence. The real-time PCR analysis confirmed this speculation. These results in the study demonstrated that the TYR-based reporter could be used to monitor miR-9 expression during DNA methylation regulation and noninvasively detect other miRNA expression and biological processes in the future.

3 days (Figures 6C and 6D). To confirm that the reduced photoacoustic signal was due to the activation of miR-9 *in vivo*, we isolated the cell-incorporated Matrigels from both flanks of mice and subjected them to real-time PCR analysis of miR-9 expression (Figure 6E). The results demonstrated that the expression level of miR-9 in the right flank was about 3.2-fold higher than that in the left flank of mice, indicating that miR-9 was really activated after 5-Aza-dC treatment, which in turn led to the decrease in photoacoustic signal.

DISCUSSION

In this study, we have successfully developed a TYR-based reporter gene for visualizing miR-9 expression during the DNA methylation regulation *in vitro* and *in vivo*. To our best knowledge, this is the first study to employ the TYR reporter gene for noninvasive PAI of miRNA expression in living organisms. Owing to the increasing role of miRNAs in the regulation of various biological processes including cell proliferation, differentiation, and tumorigenesis, the TYR-based miRNA reporter gene will be a useful tool for monitoring the localization and expression of miRNAs in diverse physiology conditions in a noninvasive manner.

Currently, there are various bioluminescence and fluorescence probes, such as luciferase gene or MBs, to detect miRNA biogenesis and function during neurogenesis and myogenesis.^{16–18} Although these optical probes provide a superior method for imaging miRNA expression, they are limited in the depth imaging with great sensitivity. Moreover, MB usually suffers from high autofluorescence back-

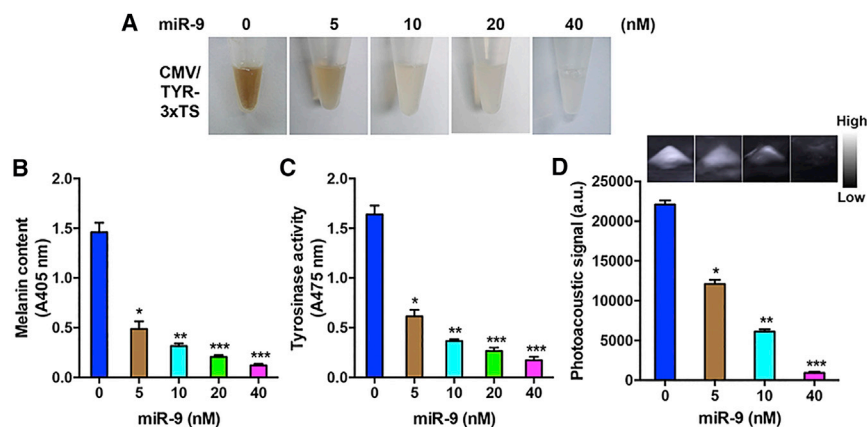


Figure 4. Repressed Activity of TYR in Response to Exogenous miR-9

Different concentrations of exogenous miR-9 (0, 5, 10, 20, 40 nM) and 4 μ g of CMV/TYR-3xTS plasmids were co-transfected in 293 cells. The cells were harvested to examine the (A) color change, (B) melanin content, (C) tyrosinase activity, and (D) photoacoustic intensity. Data are presented as means \pm SD (* p < 0.05, ** p < 0.01, *** p < 0.001 compared with control).

Real-Time PCR

Total RNAs were isolated from A549 cells that were treated with different concentrations of 5-Aza-dC using TRIzol reagent (Invitrogen). The cDNA synthesis was performed using the

One Step PrimeScript miRNA cDNA Synthesis Kit (TaKaRa, Japan) according to the manufacturer's protocols. Then the real-time PCR was carried out in triplicate using the SYBR Premix Ex TaqII (TaKaRa, Japan) in the ABI 7700 PCR system (Applied Biosystems, USA). The U6 small nuclear RNA (snRNA) was used as the internal control to normalize the miR-9 expression level. The primer sequences for miRNA-9 and U6 snRNA are as follows: miRNA-9 forward: 5'-TCT TTG GTT ATC TAG CTG TAT GA-3'; U6 forward: 5'-CAG GGG CCA TGC TAA ATC TTC-3'; U6 reverse: 5'-CTT CGG CAG CAC ATA TAC TAA AAT-3'. The reverse primer for miRNA-9 is the universal primer in the kit (Uni-miR qPCR primer).

In conclusion, the TYR-based reporter gene was successfully developed to visualize miR-9 activity regulated by DNA methylation in living cells and animals. During DNA methylation of A549 cells treated by 5-Aza-dC, the CMV/TYR-3xTS reporter demonstrated a gradual decrease in melanin content, TYR activity, and photoacoustic signal caused by the gradual activation of miR-9 expression. The TYR-based reporter could be used as a new miRNA imaging system for monitoring the dynamic expression pattern of miRNAs involved in various cellular processes and disease progression in living organisms.

MATERIALS AND METHODS

Construction of TYR and TYR-3xTS Reporters

cDNA encoding human TYR (NM_000372) in the GV140 vector was purchased from Shanghai GeneChem Technologies (Shanghai, China). TYR DNA was amplified by PCR, and the resulting TYR cDNA was inserted into the NheI and BamHI multiple cloning sites of the pcDNA 3.1 (+) vector (Invitrogen, Carlsbad, CA, USA) to get the pcDNA3.1-TYR reporter. To get the pcDNA3.1-TYR-3xTS reporter, we synthesized an oligonucleotide containing 3xTS against miR-9 (Shanghai Generay Biotech) and inserted it into the EcoRI and XhoI sites of the pcDNA3.1-TYR vector. Finally, the recombinant plasmids pcDNA3.1-TYR and pcDNA3.1-TYR-3xTS were confirmed by DNA sequencing. The sequence of the 3xTS was listed as follows: 5'-TCA TAC AGC TAG ATA ACC AAA GAT AGT ATC ATA CAG CTA GAT AAC CAA AGA TAG TAT CAT ACA GCT AGA TAA CCA AAG A-3'.

Cell Culture and Transfection

The human embryonic kidney cell line HEK293 and NSCLC cell line A549 were obtained from the Cell Bank of the Chinese Academy of Sciences (Beijing, China). Cells were cultured in DMEM (GIBCO, Carlsbad, CA, USA) supplemented with 10% fetal bovine serum (GIBCO) and 100 U/mL penicillin/streptomycin (GIBCO) at 37°C under 5% CO₂ humidified incubator. For the transfection, 293 or A549 cells were seeded in a 24-well plate and cultured overnight. The next day, cells were transfected with plasmid pcDNA3.1-TYR, pcDNA3.1-TYR-3xTS, or miRNA oligos using Lipofectamine 2000 according to the manufacturer's instructions (Invitrogen, Carlsbad, CA, USA).

Cellular Melanin Content Measurement

The cells were pretreated with 2 mM L-tyrosine for 24 hr, then harvested by centrifuge and washed three times with PBS. Then the cell pellets were sonicated and lysed with 100 μ L of NaOH (1 M) at room temperature. The cell extracts were then transferred into 96-well plates, and the melanin content of each sample was determined by measuring their absorbance at 405 nm using a multi-mode plate reader (Synergy 2; BioTek, Winooski, VT, USA).

Cellular TYR Activity Measurement

Cells in a 96-well plate were washed three times with PBS and lysed with 50 μ L of NaOH (1 M). Then 50 μ L of 2 mg/mL L-DOPA was added to each well. The final mixture was incubated at 37°C for 15 min. The absorbance of the reaction mixtures was measured using a multi-mode plate reader (Synergy 2; BioTek, Winooski, VT, USA) at 475 nm.

In Vitro Cellular PAI and Image Analysis

The *in vitro* PAI assays were performed using a multispectral photoacoustic tomography system (MSOT) with MSOT inVision 128 system (iThera Medical, Munich, Germany) as described previously with some modifications.¹⁵ This system provides two imaging approaches. One approach employs a simple handheld PAI probe, whereas the other employs a commercial phantom. We employed the handheld imaging probe approach in this study. In brief, the cells were transfected with plasmid or RNA and were harvested in PCR

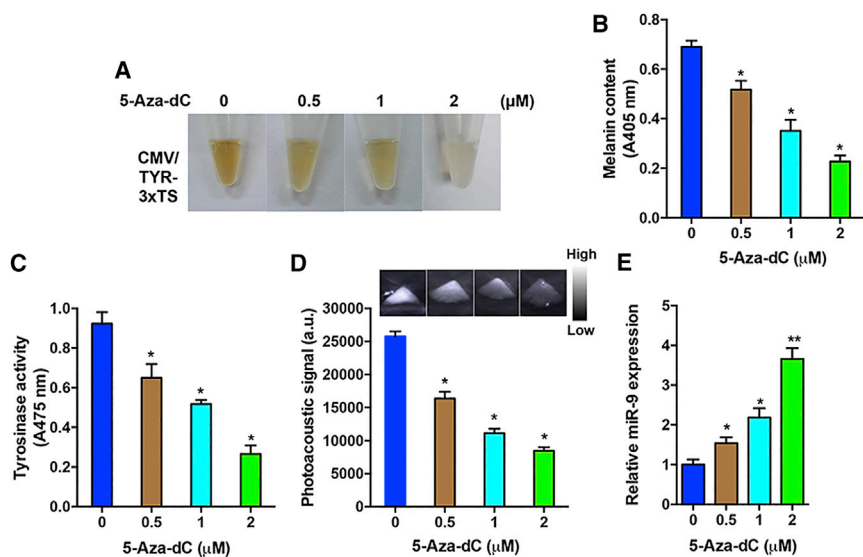


Figure 5. Monitor Endogenous miR-9 Exposure to 5-Aza-dC Treatment

A549 cells were transfected with the CMV/TYR-3xTS and further treated with different concentrations (0, 0.5, 1, 2 μM) of 5-Aza-dC for 72 hr. The cells were then harvested to examine the (A) color change, (B) melanin content, (C) tyrosinase activity, and (D) photoacoustic intensity. (E) Real-time PCR analysis of the miR-9 expression using the total RNA isolated from the cells treated with different doses of 5-Aza-dC as above. Data are presented as means ± SD (*p < 0.05; **p < 0.01 compared with control).

tubes. Then a handheld PAI probe was used to acquire photoacoustic signal at the bottom of the PCR tubes. The photoacoustic signal was acquired by the MSOT.

In Vivo PAI and BLI of Mice

All animal studies were carried out according to the Guide for the Care and Use of Laboratory Animals approved by Xidian University. Female athymic nude mice (4–6 weeks, n = 3) were obtained from the animal center of Xi'an Jiaotong University. The A549 cells

were co-transfected with CMV/TYR-3xTS and pGL3-control (Promega) luciferase plasmids. At 24 hr after transfection, the cells were harvested in 100 μL of PBS. Then the cells (5 × 10⁶ cells) were resuspended in 5-Aza-dC (2 mg/kg) and 100 μL of Matrigel, and then implanted into both flanks of mice. The cells implanted in the left flank, as a control, received no 5-Aza-dC treatment. The cells implanted in the right flank of mice were treated with 5-Aza-dC (2 mg/kg). After 72 hr of implantation, for *in vivo* imaging, mice were anesthetized with 2% isoflurane in oxygen and placed with lateral position. PAI was carried out using the same MSOT as the *in vitro* study. BLI was performed using an IVIS spectrum (Xenogen, Alameda, CA, USA) after intraperitoneal injection of D-luciferin (150 mg/kg) into mice. Image analysis was performed on the ROI using ImageJ software for quantification analysis of the

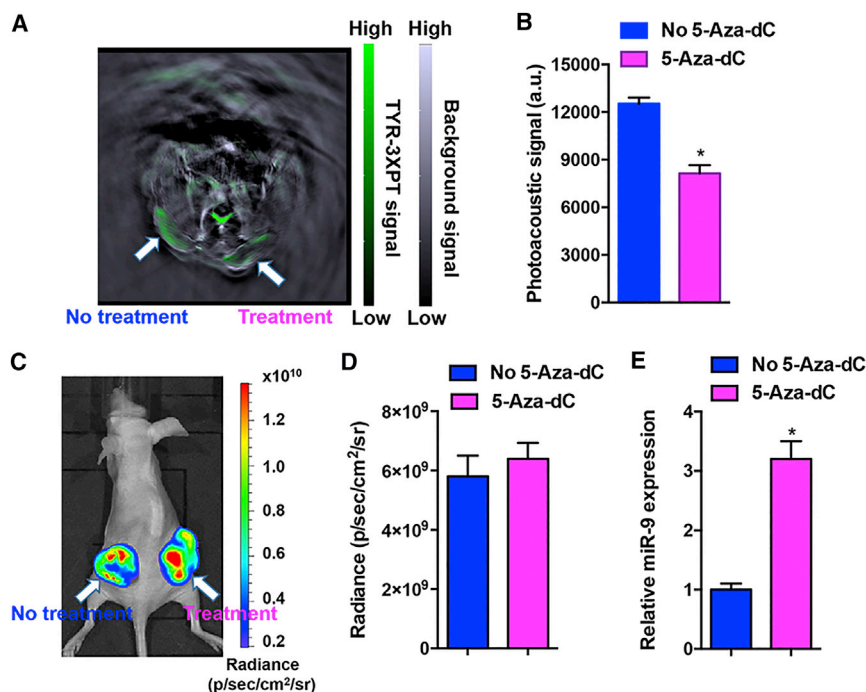


Figure 6. In Vivo Imaging of miR-9 during Epigenetic Gene Regulation

The CMV/TYR-3xTS was co-transfected into A549 cells with pGL3-control plasmid. The A549 cells treated either without or with 5-Aza-dC were implanted into the left flank and right flank of the mice (n = 3). Then (A) photoacoustic imaging and (C) bioluminescence imaging were performed after 3 days. (B and D) Quantification analysis of (B) photoacoustic signals and (D) bioluminescence signals from region of interest (ROI) in the left and right flanks. (E) Real-time PCR analysis of miR-9 expression from the total RNA isolated from the cell-incorporated Matrigels from both flanks of mice. Data are presented as means ± SD (*p < 0.05).

PAI signal intensity or Living Imaging Software 4.1 for analysis of BLI signal intensity.

Statistics Analysis

All data are presented as the mean \pm SD. Statistical analysis was performed using the Student's *t* test. A 95% confidence level was considered as the significance of differences between groups, with $p < 0.05$ indicating statistical significance.

AUTHOR CONTRIBUTIONS

Conceptualization, F.W.; Methodology, H.Z., L.Z., and Y.S.; Investigation, H.Z., L.Z., and Y.S.; Writing – Original Draft, F.W.; Writing – Review & Editing, F.W. and J.T.; Supervision, F.W. and J.T.; Funding Acquisition, F.W.

CONFLICTS OF INTEREST

No potential conflicts of interest were disclosed.

ACKNOWLEDGMENTS

This work was supported by the National Natural Science Foundation of China (grants 81571721 and 81772010) and Natural Science Basis Research Plan in Shaanxi Province of China (Program No. 2016JM8016).

REFERENCES

- Bartel, D.P. (2004). MicroRNAs: genomics, biogenesis, mechanism, and function. *Cell* 116, 281–297.
- He, L., and Hannon, G.J. (2004). MicroRNAs: small RNAs with a big role in gene regulation. *Nat. Rev. Genet.* 5, 522–531.
- Lu, J., Getz, G., Miska, E.A., Alvarez-Saavedra, E., Lamb, J., Peck, D., Sweet-Cordero, A., Ebert, B.L., Mak, R.H., Ferrando, A.A., et al. (2005). MicroRNA expression profiles classify human cancers. *Nature* 435, 834–838.
- He, L., Thomson, J.M., Hemann, M.T., Hernando-Monge, E., Mu, D., Goodson, S., Powers, S., Cordon-Cardo, C., Lowe, S.W., Hannon, G.J., and Hammond, S.M. (2005). A microRNA polycistron as a potential human oncogene. *Nature* 435, 828–833.
- Krichevsky, A.M., Sonntag, K.C., Isacson, O., and Kosik, K.S. (2006). Specific microRNAs modulate embryonic stem cell-derived neurogenesis. *Stem Cells* 24, 857–864.
- Laios, A., O'Toole, S., Flavin, R., Martin, C., Kelly, L., Ring, M., Finn, S.P., Barrett, C., Loda, M., Gleeson, N., et al. (2008). Potential role of miR-9 and miR-223 in recurrent ovarian cancer. *Mol. Cancer* 7, 35.
- Selcuklu, S.D., Donoghue, M.T., Rehmet, K., de Souza Gomes, M., Fort, A., Kovvuru, P., Muniyappa, M.K., Kerin, M.J., Enright, A.J., and Spillane, C. (2012). MicroRNA-9 inhibition of cell proliferation and identification of novel miR-9 targets by transcriptome profiling in breast cancer cells. *J. Biol. Chem.* 287, 29516–29528.
- Heller, G., Weinzierl, M., Noll, C., Babinsky, V., Ziegler, B., Altenberger, C., Minichsdorfer, C., Lang, G., Döme, B., End-Pfützenreuter, A., et al. (2012). Genome-wide miRNA expression profiling identifies miR-9-3 and miR-193a as targets for DNA methylation in non-small cell lung cancers. *Clin. Cancer Res.* 18, 1619–1629.
- Lujambio, A., and Esteller, M. (2007). CpG island hypermethylation of tumor suppressor microRNAs in human cancer. *Cell Cycle* 6, 1455–1459.
- Herman, J.G., and Baylin, S.B. (2003). Gene silencing in cancer in association with promoter hypermethylation. *N. Engl. J. Med.* 349, 2042–2054.
- Lujambio, A., Calin, G.A., Villanueva, A., Ropero, S., Sánchez-Céspedes, M., Blanco, D., Montuenga, L.M., Rossi, S., Nicoloso, M.S., Faller, W.J., et al. (2008). A microRNA DNA methylation signature for human cancer metastasis. *Proc. Natl. Acad. Sci. USA* 105, 13556–13561.
- Wang, F., Niu, G., Chen, X., and Cao, F. (2011). Molecular imaging of microRNAs. *Eur. J. Nucl. Med. Mol. Imaging* 38, 1572–1579.
- Wang, F., Song, X., Li, X., Xin, J., Wang, S., Yang, W., Wang, J., Wu, K., Chen, X., Liang, J., et al. (2013). Noninvasive visualization of microRNA-16 in the chemoresistance of gastric cancer using a dual reporter gene imaging system. *PLoS ONE* 8, e61792.
- Krumholz, A., Vanvickel-Chavez, S.J., Yao, J., Fleming, T.P., Gillanders, W.E., and Wang, L.V. (2011). Photoacoustic microscopy of tyrosinase reporter gene in vivo. *J. Biomed. Opt.* 16, 080503.
- Peng, D., Du, Y., Shi, Y., Mao, D., Jia, X., Li, H., Zhu, Y., Wang, K., and Tian, J. (2016). Precise diagnosis in different scenarios using photoacoustic and fluorescence imaging with dual-modality nanoparticles. *Nanoscale* 8, 14480–14488.
- Kang, W.J., Cho, Y.L., Chae, J.R., Lee, J.D., Choi, K.J., and Kim, S. (2011). Molecular beacon-based bioimaging of multiple microRNAs during myogenesis. *Biomaterials* 32, 1915–1922.
- Kang, W.J., Cho, Y.L., Chae, J.R., Lee, J.D., Ali, B.A., Al-Khedhairi, A.A., Lee, C.H., and Kim, S. (2012). Dual optical biosensors for imaging microRNA-1 during myogenesis. *Biomaterials* 33, 6430–6437.
- Lee, J.Y., Kim, S., Hwang, D.W., Jeong, J.M., Chung, J.K., Lee, M.C., and Lee, D.S. (2008). Development of a dual-luciferase reporter system for in vivo visualization of MicroRNA biogenesis and posttranscriptional regulation. *J. Nucl. Med.* 49, 285–294.
- Zhang, H.F., Maslov, K., Stoica, G., and Wang, L.V. (2006). Functional photoacoustic microscopy for high-resolution and noninvasive in vivo imaging. *Nat. Biotechnol.* 24, 848–851.
- Cox, B., Laufer, J.G., Arridge, S.R., and Beard, P.C. (2012). Quantitative spectroscopic photoacoustic imaging: a review. *J. Biomed. Opt.* 17, 061202.
- Oh, J.T., Li, M.L., Zhang, H.F., Maslov, K., Stoica, G., and Wang, L.V. (2006). Three-dimensional imaging of skin melanoma in vivo by dual-wavelength photoacoustic microscopy. *J. Biomed. Opt.* 11, 34032.
- Wang, Y., Maslov, K., Zhang, Y., Hu, S., Yang, L., Xia, Y., Liu, J., and Wang, L.V. (2011). Fiber-laser-based photoacoustic microscopy and melanoma cell detection. *J. Biomed. Opt.* 16, 011014.
- Paproski, R.J., Heinmiller, A., Wachowicz, K., and Zemp, R.J. (2014). Multi-wavelength photoacoustic imaging of inducible tyrosinase reporter gene expression in xenograft tumors. *Sci. Rep.* 4, 5329.
- Paproski, R.J., Forbrich, A.E., Wachowicz, K., Hitt, M.M., and Zemp, R.J. (2011). Tyrosinase as a dual reporter gene for both photoacoustic and magnetic resonance imaging. *Biomed. Opt. Express* 2, 771–780.
- Qin, C., Cheng, K., Chen, K., Hu, X., Liu, Y., Lan, X., Zhang, Y., Liu, H., Xu, Y., Bu, L., et al. (2013). Tyrosinase as a multifunctional reporter gene for Photoacoustic/MRI/PET triple modality molecular imaging. *Sci. Rep.* 3, 1490.
- Feng, H., Xia, X., Li, C., Song, Y., Qin, C., Zhang, Y., and Lan, X. (2015). TYR as a multifunctional reporter gene regulated by the Tet-on system for multimodality imaging: an in vitro study. *Sci. Rep.* 5, 15502.